Spin Hall magnetoresistance at Pt/CoFe2O4 interfaces and texture effects

Miren Isasa, Amilcar Bedoya-Pinto, Saül Vélez, Federico Golmar, Florencio Sánchez, Luis E. Hueso, Josep Fontcuberta, and Fèlix Casanova

Citation: Applied Physics Letters **105**, 142402 (2014); doi: 10.1063/1.4897544
View online: http://dx.doi.org/10.1063/1.4897544
View Table of Contents: http://scitation.aip.org/content/aip/journal/apl/105/14?ver=pdfcov
Published by the AIP Publishing

Spin Hall magnetoresistance at Pt/$CoFe_2O_4$ interfaces and texture effects

Miren Isasa,[1] Amilcar Bedoya-Pinto,[1] Saül Vélez,[1] Federico Golmar,[1,2,3] Florencio Sánchez,[4] Luis E. Hueso,[1,5] Josep Fontcuberta,[4] and Fèlix Casanova[1,5]
[1]*CIC nanoGUNE, 20018 Donostia-San Sebastian, Basque Country, Spain*
[2]*I.N.T.I.-CONICET, Av. Gral. Paz 5445, Ed. 42, B1650JKA, San Martín, Bs. As., Argentina*
[3]*ECyT, UNSAM, Martín de Irigoyen 3100, B1650JKA, San Martín, Bs. As., Argentina*
[4]*Institut de Ciència de Materials de Barcelona (ICMAB-CSIC), Campus UAB, 08193 Bellaterra, Catalonia, Spain*
[5]*IKERBASQUE, Basque Foundation for Science, 48011 Bilbao, Basque Country, Spain*

(Received 9 June 2014; accepted 20 September 2014; published online 8 October 2014)

We report magnetoresistance measurements on thin Pt bars grown on epitaxial (001) and (111) $CoFe_2O_4$ (CFO) ferrimagnetic insulating films. The results can be described in terms of the recently discovered spin Hall magnetoresistance (SMR). The magnitude of the SMR depends on the interface preparation conditions, being optimal when the Pt/CFO samples are prepared *in situ*, in a single process. The spin-mixing interface conductance, the key parameter governing SMR and other relevant spin-dependent phenomena, such as spin pumping or spin Seebeck effect, is found to be different depending on the crystallographic orientation of CFO, highlighting the role of the composition and density of magnetic ions at the interface on spin mixing. © *2014 AIP Publishing LLC*. [http://dx.doi.org/10.1063/1.4897544]

Spintronics exploits the spin-dependent charge transport in solids. Pure spin currents, in which spin angular momentum with no electric charge is transported, are expected to lead to a new generation of faster and low-energy consumption spintronic devices.[1] Several methods to create pure spin currents have been developed in the recent years, including non-local spin injection,[2–4] spin pumping,[5–7] direct spin Hall effect (SHE),[7,8] or spin Seebeck effect.[9–12] The detection of these pure spin currents can be done via the inverse spin Hall effect (ISHE).[8,13] Platinum is the most commonly used non-magnetic metal (NM) for spin current to charge current conversion.[6–9,11,14]

Spin currents, in the form of spin wave excitations, can propagate in ferromagnetic insulators (FMI) for long distances. NM/FMI bilayers are used to create (*via* SHE) and/or detect them (*via* ISHE).[11,14] Within this framework, a new type of magnetoresistance, so called "spin Hall magnetoresistance" (SMR), has been recently discovered in Pt/YIG.[15–20] As sketched in Fig. 1, SMR arises from the simultaneous effect of SHE and ISHE in the NM (Fig. 1(a)), combined with the presence of a FMI in one of the interfaces. The generated spin current can be absorbed by the magnetization **M** as a spin-transfer torque when **M** is perpendicular to **s** (Fig. 1(b)), where **s** is the spin polarization, or reflected when **M** and **s** are parallel (Fig. 1(c)). Therefore, the charge current in the NM layer varies and its resistance will depend on the magnetization direction at the surface of the FMI. So far, SMR has only been reported for NM/FMI being FMI soft ferromagnets such as YIG[16–19] and more recently Fe_3O_4 and $NiFe_2O_4$.[20]

The concept of spin-mixing conductance,[21] which determines the efficiency of the spin current transport at the interface, is at the base not only of SMR but also of spin Seebeck effect and spin pumping.[22] The nature of the NM/FMI interface strongly affects the observation of such phenomena.[17,23–26] A detailed comprehension of the mechanisms behind the spin-mixing conductance concept is thus important for a better understanding and control of all these spin-dependent effects. Instrumental for the purpose of this research, we select $CoFe_2O_4$ (CFO), a room-temperature ferrimagnetic insulating oxide.[27] The presence of Co^{2+} ions anticipates a large magnetic anisotropy in CFO (Ref. 28) and the competing nature of magnetic interactions in spinels may lead to different magnetic properties[29] at (001) and (111) surfaces. Therefore, CFO is especially suitable to explore the role of the surface magnetic textures by using SMR. In this work, we report magnetoresistance measurements on Pt layers grown on (001) or (111) epitaxial CFO films, displaying features fully compatible with SMR, with different spin-mixing conductances for (001) and (111) interfaces. This observation is in agreement with recent speculations that spin-mixing conductance anisotropy in ferrimagnetic spinels could be larger than in YIG.[21,30]

CFO films were grown on (001) and (111) $SrTiO_3$ (STO) substrates. The deposition was carried using a CFO stoichiometric target by pulsed laser deposition using a KrF laser with fluence of 1.5(3) J/cm^2 and a repetition rate of 5 Hz at a temperature of about 550 °C and oxygen pressure $P_{O2} = 0.1$ mbar.[31] The thickness of the CFO films ranged from 40 nm to 67 nm (see Table I), as inferred from growth rate calibration by X-ray reflectometry.[27] A total of five pairs of Pt/CFO samples were prepared by using two substrate orientations: STO(001) and STO(111), and three distinct processes denoted: EX-1, EX-2, and IN (Table I). In samples prepared by processes EX-2 and IN, the CFO layers were grown simultaneously on (001) and (111) substrates in each run, whereas the Pt layer, deposited by dc sputtering, was grown either *ex-situ* (EX-2) or *in-situ* (IN). In process EX-1, the CFO layers on (001) and (111) substrates were grown in different runs and the Pt layer *ex-situ*. For EX-1 and EX-2 samples, the thickness of Pt was kept constant (around 7 nm). In case of IN samples, Pt of different thicknesses

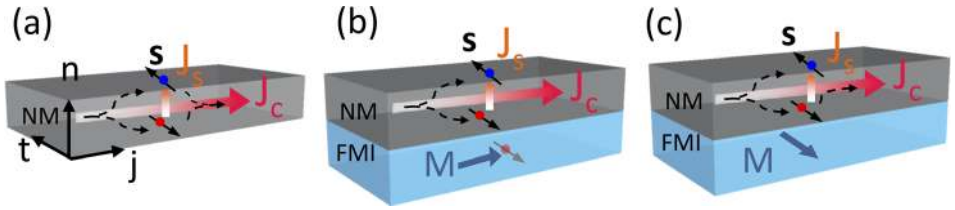

FIG. 1. (a) NM layer with strong spin-orbit coupling, with a charge current $\mathbf{j}_c$ flowing along $\mathbf{j}$. A spin current $\mathbf{j}_s$ along $\mathbf{n}$ with spin polarization $\mathbf{s}$ along $\mathbf{t}$ is created due to SHE. The spin current is reflected back at the surfaces, generating additional charge current due to ISHE. (b) NM/FMI bilayer where the magnetization in the FMI is perpendicular to the spin polarization of the spin current. In this case, the spin current will be absorbed at the NM/FMI interface. (c) When the magnetization is parallel to the spin polarization, the spin current will be reflected. The difference in resistance between (b) and (c) leads to SMR.

were grown (6.5, 4, and 2 nm). The Pt layers in the *ex-situ* processes EX-1 and EX-2 were deposited at room temperature whereas in the *in-situ* IN process, the Pt was grown at 400 °C. For the transport measurements, the Pt layers were patterned into Hall bars (width $W = 100\,\mu m$ and length $L = 800\,\mu m$), as sketched in Fig. 2. For EX-1 and EX-2, patterning was done by using electron-beam lithography with positive resist followed by dc sputtering of the Pt and lift-off, fabricated on top of the CFO films. The Pt layers of IN samples were patterned by using electron-beam lithography with negative resist followed by Ar-ion milling and resist removal. A sample of Pt/YIG was also grown for control experiments using a commercial (111) YIG films. Magnetotransport measurements were performed at 300 K in a cryostat with external magnetic fields ($\mathbf{H}$) ranging from −9 T to 9 T applied at different angles. Two different configurations, longitudinal and transverse (see sketches in Fig. 2), have been used for the electrical measurements.

The presence of SMR is assessed by performing angle-dependent magnetoresistance (ADMR) measurements. In Fig. 2, we show, as illustrative examples, the longitudinal and transverse ADMR measured for (001)EX-1(7) and (111)EX-2(7) samples, measured at 9 T, in three relevant $\mathbf{H}$-rotation planes defined in sketches of Fig. 2. Baseline resistances of $R_{L0} = 338\ \Omega$ (Figs. 2(a)–2(c)) and $R_{L0} = 763\ \Omega$ (Figs. 2(e)–2(g)) for the longitudinal configuration and $R_{T0} = 24.7\,m\Omega$ (Fig. 2(d)) and $R_{T0} = 824\,m\Omega$ (Fig. 2(h)) for the transverse configuration have been subtracted for clarity. According to the current understanding of SMR,[15,16,20] the angular dependence of the longitudinal resistivity ρ_L and the transverse resistivity ρ_T measured in the NM layer are given by

$$\rho_L = \rho_0 + \rho_1(1 - m_t^2), \tag{1}$$

$$\rho_T = \rho_2 m_n + \rho_3 m_j m_t, \tag{2}$$

where $\mathbf{m}(m_j, m_t, m_n) = \mathbf{M}/M_s$ are the cosine directors of the magnetization $\mathbf{M}$ along the $\mathbf{j}$-, $\mathbf{t}$-, and $\mathbf{n}$-directions; M_s is the saturation magnetization of CFO; ρ_0 is the baseline resistivity of the NM layer; ρ_1/ρ_0 is the SMR; and ρ_2 accounts for an anomalous Hall-like contribution. According to this theoretical model, $\rho_3 = \rho_1$.[15,16,20] As the measurements shown in Fig. 2 have been performed at fields (9 T) much larger than the coercive field H_C of the CFO film and where the film-magnetization is reversible,[27] we assume that $\mathbf{m}$ roughly follows $\mathbf{H}$, i.e., $\mathbf{m}||\mathbf{H}$.

The longitudinal resistance $R_L(\gamma)$ (Figs. 2(a) and 2(e)) does not show any angular dependence, therefore an anisotropic magnetoresistance ($AMR \approx \cos^2\gamma$) (Ref. 32) of Pt, induced by proximity effect[33] of the neighboring ferromagnetic CFO layer, is excluded. In contrast, a constant $R_L(\gamma)$ is in agreement with Eq. (1). $R_L(\beta)$, plotted in Figs. 2(b) and 2(f), can be described by $R_L(\beta) \approx \cos^2\beta$. This dependence agrees also with the SMR prediction (Eq. (1)) (with $\rho_1 > 0$). Similarly, $R_L(\alpha)$ data shown in Figs. 2(c) and 2(g) can also be described by $R_L(\alpha) \approx \cos^2\alpha$. In this configuration, both AMR (Ref. 32) and SMR (Eq. (1)) might contribute but, as argued above, AMR has been found to be negligible and thus the observed α-dependence can be safely ascribed to SMR. The transverse resistance $R_T(\alpha)$, shown in Figs. 2(d) and 2(h), displays a $\cos\alpha \times \sin\alpha$ dependence, fully consistent

TABLE I. Summary of relevant data corresponding to the five pairs of Pt/CFO samples used in this work: fabrication process, crystallographic orientation of CFO film, thickness of CFO film (t_{CFO}), thickness of Pt film (t_{Pt}), resistivity of the Pt film (ρ_0), SMR effect ($\rho_1/\rho_0 = \Delta R_L/R_{L0}$), and the real part of the spin-mixing conductance (G_r) calculated from Eq. (3) by using $\theta_{SH,Pt} = 0.056$ and $\lambda_{Pt} = 3.4$ nm.[35]

Sample	Fabrication process	Crystallographic orientation	t_{CFO} (nm)	t_{Pt} (nm)	ρ_0 ($\mu\Omega$ cm)	$\Delta R_L/R_{L0}$	G_r ($\Omega^{-1}m^{-2}$)
(001) EX-1(7)	EX-1	(001)	67	7	29.6	2.7×10^{-4}	2.4×10^{14}
(111) EX-1(7)	EX-1	(111)	56	7	19.5	0.2×10^{-4}	1.4×10^{13}
(001) EX-2(7)	EX-2	(001)	57	7	29.7	1.2×10^{-4}	7.4×10^{13}
(111) EX-2(7)	EX-2	(111)	57	7	66.8	0.9×10^{-4}	2.4×10^{13}
(001) IN(7)	IN	(001)	40	6.5	21.4	2.5×10^{-4}	2.4×10^{14}
(111) IN(7)	IN	(111)	40	6.5	18.2	1.8×10^{-4}	1.9×10^{14}
(001) IN(4)	IN	(001)	40	4	20.2	3.4×10^{-4}	2.6×10^{14}
(111) IN(4)	IN	(111)	40	4	23.3	2.5×10^{-4}	1.4×10^{14}
(001) IN(2)	IN	(001)	40	2	36.0	6.0×10^{-4}	2.4×10^{14}
(111) IN(2)	IN	(111)	40	2	34.5	4.3×10^{-4}	1.1×10^{14}

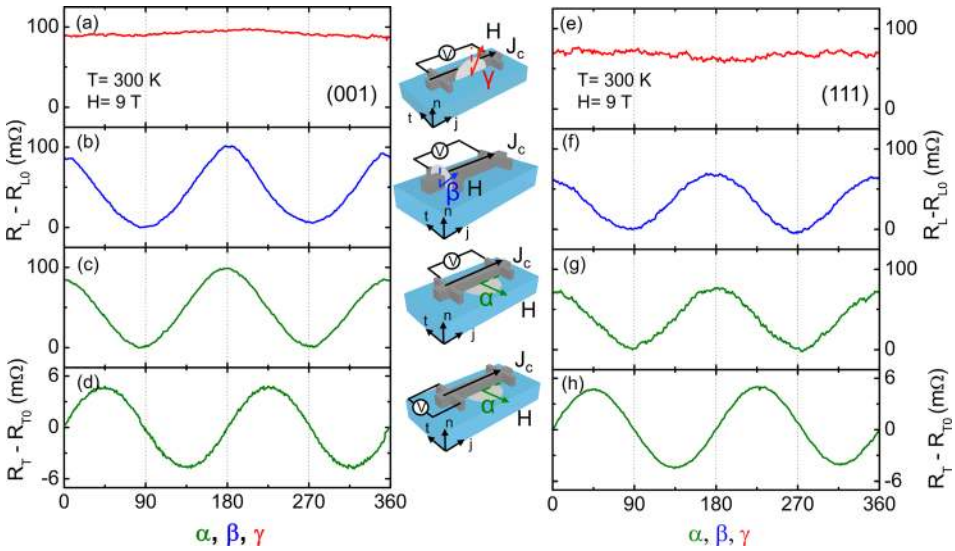

FIG. 2. Angle-dependent magnetoresistance measurements at 9 T and 300 K for (001)EX-1(7) ((a)–(d)) and (111)EX-2(7) ((e)–(h)) samples. $R_{L,T}$ is the measured resistance and $R_{L0,T0}$ is the subtracted background. ((a)–(c) and (e)–(g)) Longitudinal resistance R_L as a function of the direction of the applied magnetic field, in three different rotation planes. ((d) and (h)) Transverse resistance R_T as a function of angle α. Central panel: sketches indicate the definition of the angles α, β, γ and the measurement configuration.

with Eq. (2). In summary, the observed ADMR response of the (001)EX-1(7) and (111)EX-2(7) samples indicates the prevalence of SMR in Pt/CFO with both epitaxial (001) and (111) CFO textures.

The amplitude of the angular variation of the longitudinal resistance for the (001)EX-1(7) sample is $\Delta R_L = 90\,m\Omega$ and thus SMR is $\rho_1/\rho_0 = \Delta R_L/R_{L0} = 2.7 \times 10^{-4}$. The change in the transverse resistance ($\Delta R_T = 9.22\,m\Omega$) is smaller than ΔR_L by ~10, in agreement with the difference on the geometrical factor ($L/W \sim 8$), and yields the expected $\rho_1 = \rho_3$ relation.[15,16,20] The magnitude of SMR is given by[15,16]

$$\frac{\rho_1}{\rho_0} \approx \theta_{SH,NM}^2 \frac{\frac{2\lambda_{NM}^2}{\sigma_{NM} t_{NM}} G_r \tanh^2 \frac{t_{NM}}{2\lambda_{NM}}}{1 + \frac{2\lambda_{NM}}{\sigma_{NM}} G_r \coth \frac{t_{NM}}{\lambda_{NM}}}, \quad (3)$$

where σ_{NM}, λ_{NM}, $\theta_{SH,NM}$, and t_{NM} are the conductivity, spin diffusion length, spin Hall angle, and thickness of the NM element (Pt), respectively, and G_r is the real part of the spin-mixing conductance at the Pt/CFO interface. G_r governs the spin transfer torque at the interface and thus the efficiency of spin injection.[21,23,26] G_r can be extracted from the magnitude of the SMR using Eq. (3), if the other parameters are known. The discrepancy in the values of $\theta_{SH,Pt}$ and λ_{Pt} existing in the literature[34] has been clarified very recently[35] and, accordingly, we will use the values $\theta_{SH,Pt} = 0.056$ and $\lambda_{Pt} = 3.4\,nm$ given in Ref. 35. For the (001)EX-1(7) sample, we get $G_r = 2.4 \times 10^{14}$ $\Omega^{-1}m^{-2}$, which is similar to values reported in literature for other NM/FMI systems; indeed, for Pt/YIG, it ranges from 1.2×10^{12} to 1.3×10^{15} $\Omega^{-1}m^{-2}$,[14,16–20,22,24,26,36] 1.9×10^{14} $\Omega^{-1}m^{-2}$ for Au/YIG (Ref. 23) or 2.6×10^{14} $\Omega^{-1}m^{-2}$ for Pt/Fe_3O_4.[37] A detailed comparison between our results and previous works is difficult due to the use of different set of $\theta_{SH,Pt}$, λ_{Pt} parameters for the calculation of G_r, and different fabrication conditions. A more direct comparison could be done with the magnitude of SMR: our result lies within the range of values from 1.9×10^{-4} to 9.5×10^{-4} obtained for Pt/YIG with similar Pt thicknesses,[16,17,20] but also in this case the different fabrication conditions seem to influence the SMR value. For example, a control experiment in a Pt/YIG sample fabricated by the same EX-1 process gives us $\rho_1/\rho_0 = \Delta R_L/R_{L0} = 0.7 \times 10^{-4}$.[27] Of higher interest for the purpose of this paper, however, is the comparison between the G_r of Pt/(001)CFO and Pt/(111)CFO samples. It can be observed in Figs. 2(f) and 2(g) that, for the (111)EX-2(7) sample, the change in longitudinal resistance ($\Delta R_L = 69\,m\Omega$) and the spin Hall magnetoresistance term $\rho_1/\rho_0 = \Delta R_L/R_{L0} = 0.9 \times 10^{-4}$ are smaller than for the (001)EX-1(7) sample. This leads to a smaller $G_r = 2.4 \times 10^{13}$ $\Omega^{-1}m^{-2}$.

This result suggests that G_r depends on the relevant crystallographic planes [(001) vs (111)] forming the Pt/CFO interface. Before proceeding with the analysis of this experimental observation, we show in Table I the spin Hall magnetoresistance, at 9 T and 300 K, and the extracted G_r values for all samples, in which we have used the same set of parameters ($\theta_{SH,Pt} = 0.056$ and $\lambda_{Pt} = 3.4\,nm$ (Ref. 35)). We will first focus on the samples with Pt thickness of ~7 nm. Inspection of data in Table I immediately reveals some remarkable trends: (i) For all pair of 7-nm-thick Pt samples (IN, EX-2, and EX-1), $G_r(001)$ is different and somewhat larger than the corresponding $G_r(111)$ and (ii), although the CFO layers have been grown under nominally identical conditions in samples EX-2 and IN, the extracted spin-mixing conductance differs, being definitely larger for IN than for EX-2 samples. Regarding (ii), it is well known that G_r is very sensitive to the details of the interface between the FMI and the NM.[17,23–26] As the Pt layer is deposited differently in EX-2 and IN samples (*ex-situ* and *in-situ*, respectively), the interface is likely modified during the *ex-situ* Pt deposition, because it involves exposure of the free surface of the CFO to air and to the chemicals used for the lithography process. Consequently, it is not surprising to find a larger G_r value for IN than for EX-2 samples and therefore $G_r(001)$ and $G_r(111)$ values for IN samples set upper bounds to the spin-mixing conductances of (001) and (111) interfaces in Pt/CFO. Regarding (i), the systematic observation that for every pair of samples $G_r\,(001) > G_r\,(111)$ suggests that the spin-mixing conductance may depend on the interface orientation of the ferromagnetic insulator.

From this analysis, where pairs of samples prepared using different fabrication processes are compared, we infer

that SMR is a robust phenomenon that is present in Pt/CFO, although a quantitative comparison between crystallographic orientations can be best done for IN samples due to the optimal interface preparation conditions. For this reason, we will now focus on the samples prepared with the same IN process and different Pt thicknesses: (001)IN(2,4,7) and (111)IN(2,4,7). We show in Fig. 3 the dependence of the magnetoresistance, at 9 T and 300 K, of the three pairs of IN samples when rotating the magnetic field in a plane perpendicular to the current (i.e., as a function of β). In this geometry, the amplitude of the observed magnetoresistance ($\rho_1/\rho_0 = \Delta R_L/R_{L0}$) is linked to G_r (Eq. (3)), and it thus allows us a simple visualization of the changes of G_r and its evaluation. It can be appreciated in Table I that the extracted G_r values for these samples are radically different for both terminations [$G_r(001) = 2.5(1) \times 10^{14}\ \Omega^{-1}m^{-2}$ and $G_r(111) = 1.5(4) \times 10^{14}\ \Omega^{-1}m^{-2}$] and largely independent of the Pt thickness when considering the same crystallographic orientation. This last observation, which is expected as G_r is basically an interfacial property, demonstrates the good reproducibility of the Pt/CFO interface achieved in our fabrication IN process. Therefore, the G_r values are consistently different between orientations [$G_r(001) > G_r(111)$ for any Pt thickness], being a solid evidence of the anisotropy of the spin-mixing conductance.

Since the density of magnetic ions at the interface and their magnetic orientation determine the spin transfer, any detailed understanding for the observed difference $G_r(001) > G_r(111)$ should start by considering the microscopic nature of the atomic planes involved at the interface. This is far from obvious in spinel AB_2O_4 oxides; for instance, in (111), there are six different atomic planes all of them being polar and, therefore, unstable.[27] There are different mechanisms to solve this dipole-associated electrostatic energy divergence and, for this reason, the surface termination in (001) and (111) planes of spinel oxides is strongly dependent on the conditions used to prepare the surfaces.[27] As a result, a definitive conclusion is still missing even for the most studied case of Fe_3O_4 (see Ref. 38 for a recent review). Nevertheless, theoretical and experimental trends indicate that in (001) surfaces the termination containing tetrahedrally coordinated Fe^{3+} ions is most commonly found, whereas in (111) surfaces both oxygen and tetrahedral terminations are more favorable.[38] A similar situation has been suggested for $MgAl_2O_4$ (Ref. 39) and $CoFe_2O_4$.[40]

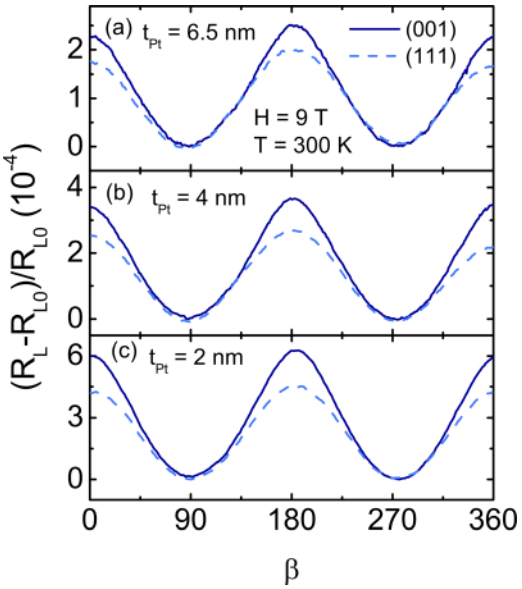

FIG. 3. Angle-dependent longitudinal magnetoresistance, at 9 T and 300 K, when rotating the magnetic field in a plane perpendicular to the current (i.e., as a function of β) for epitaxial (001) and (111) CFO/Pt samples grown *in situ* with (a) 6.5 nm, (b) 4 nm, and (c) 2 nm of Pt. R_L is the measured resistance and R_{L0} is the subtracted background.

Recently, first-principles calculations of G_r for different surfaces of $CoFe_2O_4$ (Ref. 41) predict values of $2.82 \times 10^{14}\ \Omega^{-1}m^{-2}$ for the tetrahedral termination in the case of (001) orientation and $0.63\ (1.15) \times 10^{14}\ \Omega^{-1}m^{-2}$ for the oxygen (tetrahedral) terminations in (111) orientation. The values for these stable (111) terminations are thus smaller than that predicted for the most stable (001) termination. Our experimental values are similar to these calculated values and, therefore, in agreement with the higher stability of the tetrahedrally coordinated Fe^{3+} planes in (001) and tetrahedrally coordinated Fe^{3+} and oxygen-terminated planes in (111) as argued above.

To conclude, we have shown that spin Hall magnetoresistance is at the origin of the longitudinal and transverse magnetoresistance of Pt films deposited on epitaxial (001) and (111) ferrimagnetic insulating CFO thin films. Although the observed SMR is a robust phenomenon, its magnitude depends on the interface preparation conditions, being optimal when the samples are prepared *in situ*. The spin-mixing conductance at Pt/CFO is found to be similar to those reported for other NM/FMI heterostructures. Most importantly, the observation that (001) and (111) CFO films have clearly different SMR illustrates that atomic configuration of the magnetic atoms at NM/FMI interfaces have an important effect in the spin-mixing conductance, a crucial parameter which is also at the base of other relevant spin-dependent phenomena such as spin pumping or spin Seebeck effect. These results might have important implications for the design of future spintronic devices based on insulators.

This work was supported by the European Union 7th Framework Programme under the Marie Curie Actions (256470-ITAMOSCINOM), NMP Project (263104-HINTS) and the European Research Council (Grant No. 257654-SPINTROS), by the Spanish Ministry of Science and Education (MAT2012-37638, MAT2011-29269-C03, and CSD2007-00041) by the Basque Government (PI2011-1) and by the Catalan Government (2009 SGR 00376). M.I. acknowledges the Basque Government for a Ph.D. fellowship (BFI-2011-106). J.F. acknowledges stimulating discussions with Xavier Martí.

[1]*Spin Current*, edited by S. Maekawa, S. O. Valenzuela, E. Saitoh, and T. Kimura (Oxford University Press, 2012).
[2]F. J. Jedema, A. T. Filip, and B. J. van Wees, Nature **410**, 345 (2001).
[3]F. Casanova, A. Sharoni, M. Erekhinsky, and I. K. Schuller, Phys. Rev. B **79**, 184415 (2009).
[4]E. Villamor, M. Isasa, L. E. Hueso, and F. Casanova, Phys. Rev. B **87**, 094417 (2013).
[5]Y. Tserkovnyak, A. Brataas, G. E. W. Bauer, and B. I. Halperin, Rev. Mod. Phys. **77**, 1375 (2005).

[6]E. Saitoh, M. Ueda, H. Miyajima, and G. Tatara, Appl. Phys. Lett. **88**, 182509 (2006).
[7]K. Ando, S. Takahashi, K. Harii, K. Sasage, J. Ieda, S. Maekawa, and E. Saitoh, Phys. Rev. Lett. **101**, 036601 (2008).
[8]T. Kimura, Y. Otani, T. Sato, S. Takahashi, and S. Maekawa, Phys. Rev. Lett. **98**, 156601 (2007).
[9]K. Uchida, S. Takahashi, K. Harii, J. Ieda, W. Koshibae, K. Ando, S. Maekawa, and E. Saitoh, Nature **455**, 778 (2008).
[10]A. Slachter, F. L. Bakker, J. P. Adam, and B. J. Van Wees, Nat. Phys. **6**, 879 (2010).
[11]K. Uchida, J. Xiao, H. Adachi, J. Ohe, S. Takahashi, J. Ieda, T. Ota, Y. Kajiwara, H. Umezawa, H. Kawai, G. E. W. Bauer, S. Maekawa, and E. Saitoh, Nat. Mater. **9**, 894 (2010).
[12]M. Erekhinsky, F. Casanova, I. K. Schuller, and A. Sharoni, Appl. Phys. Lett. **100**, 212401 (2012).
[13]S. O. Valenzuela and M. Tinkham, Nature **442**, 176 (2006).
[14]Y. Kajiwara, K. Harii, S. Takahashi, J. Ohe, K. Uchida, M. Mizuguchi, H. Umezawa, H. Kawai, K. Ando, K. Takanashi, S. Maekawa, and E. Saitoh, Nature **464**, 262 (2010).
[15]Y.-T. Chen, S. Takahashi, M. Althammer, S. T. B. Goennenwein, E. Saitoh, and G. E. W. Bauer, Phys. Rev. B **87**, 144411 (2013).
[16]H. Nakayama, M. Althammer, Y.-T. Chen, K. Uchida, Y. Kajiwara, D. Kikuchi, T. Ohtani, S. Geprägs, M. Opel, S. Takahashi, R. Gross, G. E. W. Bauer, S. T. B. Goennenwein, and E. Saitoh, Phys. Rev. Lett. **110**, 206601 (2013).
[17]N. Vlietstra, J. Shan, V. Castel, B. J. van Wees, and J. Ben Youssef, Phys. Rev. B **87**, 184421 (2013).
[18]C. Hahn, G. de Loubens, O. Klein, M. Viret, V. V. Naletov, and J. Ben Youssef, Phys. Rev. B **87**, 174417 (2013).
[19]N. Vlietstra, J. Shan, V. Castel, J. Ben Youssef, G. E. W. Bauer, and B. J. van Wees, Appl. Phys. Lett. **103**, 032401 (2013).
[20]M. Althammer, S. Meyer, H. Nakayama, M. Schreier, S. Altmannshofer, M. Weiler, H. Huebl, S. Geprägs, M. Opel, R. Gross, D. Meier, C. Klewe, T. Kuschel, J.-M. Schmalhorst, G. Reiss, L. Shen, A. Gupta, Y.-T. Chen, G. E. W. Bauer, E. Saitoh, and S. T. B. Goennenwein, Phys. Rev. B **87**, 224401 (2013).
[21]X. Jia, K. Lui, K. Xia, and G. E. W. Bauer, Europhys. Lett. **96**, 17005 (2011).
[22]M. Weiler, M. Althammer, M. Schreier, J. Lotze, M. Pernpeintner, S. Meyer, H. Huebl, R. Gross, A. Kamra, J. Xiao, Y.-T. Chen, H. Jiao, G. E. W. Bauer, and S. T. B. Goennenwein, Phys. Rev. Lett. **111**, 176601 (2013).
[23]C. Burrowes, B. Heinrich, B. Kardasz, E. A. Montoya, E. Girt, Y. Sun, Y.-Y. Song, and M. Wu, Appl. Phys. Lett. **100**, 092403 (2012).
[24]L. Qiu, K. Ando, K. Uchida, Y. Kajiwara, R. Takahashi, H. Nakayama, T. An, Y. Fujikawa, and E. Saitoh, Appl. Phys. Lett. **103**, 092404 (2013).
[25]Y. Ando, K. Ichiba, S. Yamada, E. Shikoh, T. Shinjo, K. Hamaya, and M. Shiraishi, Phys. Rev. B **88**, 140406(R) (2013).
[26]M. B. Jungfleisch, V. Lauer, R. Neb, A. V. Chmak, and B. Hillebrands, Appl. Phys. Lett. **103**, 022411 (2013).
[27]See supplementary material at http://dx.doi.org/10.1063/1.4897544 for a brief description of $CoFe_2O_4$ (CFO), a discussion on the surface termination (001) and (111) in spinel oxides, experimental details of CFO growth, magnetic characterization of CFO and control experiments.
[28]J. C. Slonczewski, Phys. Rev. **110**, 1341 (1958).
[29]R. H. Kodama, A. E. Berkowitz, E. J. McNiff, Jr., and S. Foner, Phys. Rev. Lett. **77**, 394 (1996).
[30]J. C. Slonczewski, Phys. Rev. B **82**, 054403 (2010).
[31]N. Dix, I. Fina, R. Bachelet, L. Fàbrega, C. Kanamadi, J. Fontcuberta, and F. Sánchez, Appl. Phys. Lett. **102**, 172907 (2013).
[32]T. R. McGuire and R. I. Potter, IEEE Trans. Magn. **11**, 1018 (1975).
[33]S. Y. Huang, X. Fan, D. Qu, Y. P. Chen, W. G. Wang, J. Wu, T. Y. Chen, J. Q. Xiao, and C. L. Chien, Phys. Rev. Lett. **109**, 107204 (2012).
[34]L. Liu, R. A. Buhrman, and D. C. Ralph, e-print arXiv:1111.3702.
[35]J.-C. Rojas-Sánchez, N. Reyren, P. Laczkowski, W. Savero, J.-P. Attané, C. Deranlot, M. Jamet, J.-M. George, L. Vila, and H. Jaffrès, Phys. Rev. Lett. **112**, 106602 (2014).
[36]V. Castel, N. Vlietstra, B. J. van Wees, and J. B. Youssef, Appl. Phys. Lett. **101**, 132414 (2012).
[37]F. D. Czeschka, L. Dreher, M. S. Brandt, M. Weiler, M. Althammer, I.-M. Imort, G. Reiss, A. Thomas, W. Schoch, W. Limmer, H. Huebl, R. Gross, and S. T. B. Goennenwein, Phys. Rev. Lett. **107**, 046601 (2011).
[38]H. Kuhlenbeck, S. Shaikhutdinov, and H.-J. Freund, Chem. Rev. **113**, 3986 (2013).
[39]W.-Z. Li, L. Kovarik, D. Mei, J. Liu, Y. Wang, and C. H. F. Peden, Nat. Commun. **4**, 2481 (2013).
[40]N. Ballarini, F. Cavani, S. Passeri, L. Pesaresi, A. F. Lee, and K. Wilson, Appl. Catal., A **366**, 184 (2009).
[41]L. Wang, K. Xia, and G. E. W. Bauer, private communication (30 July 2014).